Engineering Geology 246 (2018) 45–56

Contents lists available at ScienceDirect

Engineering Geology

journal homepage: www.elsevier.com/locate/enggeo

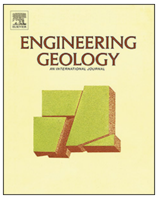

Comprehensive sandstone fracturing characterization: Integration of fiber Bragg grating, digital imaging correlation and acoustic emission measurements

Guangqing Zhang[a,*], Yuekun Xing[b], Linlin Wang[a]

[a] *State Key Laboratory of Petroleum Resources and Prospecting, China University of Petroleum, Beijing 100249, PR China*
[b] *Department of Engineering Mechanics, College of Petroleum Engineering, China University of Petroleum, Beijing 100249, PR China*

ARTICLE INFO

Keywords:
Fiber Bragg grating
Digital imaging correlation
Acoustic emission
Integrated measurement
Fracturing characteristics

ABSTRACT

Prominent characteristics of rock fracturing can be described mainly by crack opening displacement (COD), fracture process zone (FPZ) and fracture energy. In view of lack of real-time and comprehensive measurement techniques for characterizing rock fracturing in field applications, this paper developed a characterizing method of rock fracturing by utilizing and integrating Fiber Bragg Grating (FBG), Digital Imaging Correlation (DIC) and Acoustic Emission (AE). In this paper, mode I fracturing test was performed on sandstone using three-point bending, and the fracturing process was simultaneously detected and recorded by FBG, DIC and AE. The experimental results showed that (1) DIC-based measurement of horizontal displacements across the fracture presented a localized discontinuity, in accordance with FBG-based real-time measurement. At the onset of traction-free zone formation (peak load), the critical COD (δ_c) was found to be 76 μm as identified by DIC and FBG. (2) Moreover, the dissipated energy distribution and cohesive crack profile in FPZ characterized by the integrated measurement, indicated that 70%–90% of AE energy (dissipated energy) populated in the FPZ, little AE energy concentrated in the traction-free zone, and the position of δ_c delineated a boundary for specifying FPZ. The length of fully developed FPZ was 20 mm (± 2 mm) in length. (3) The integrated measurement delineated the cohesive crack, which was not available previously. The integrated measurement revealed the softening curve followed a straight line; the relationship between FPZ length and crack tip opening displacement (CTOD) was linear, and the relationship between dissipated energy and FPZ length was quadratic. Based on the interrelations of cohesive crack characteristics identified by the integrated measurements, real-time fracturing can be captured by one technique (e.g. FBG) in field application.

List of symbols

FPZ	fracture process zone
FBG	fiber Bragg grating
DIC	digital imaging correlation
AE	acoustic emission
COD	crack opening displacement
CTOD	crack tip opening displacement
CMOD	crack mouth opening displacement
3 PB	three-point bending
P	load of 3PB test
x, y, z	coordinates
x_i, y_i, z_i	AE sensor locations
t_i	the onset time received by each AE channel
t_0	the occurrence time of AE event
v	the body wave velocity of the material
f, g	the grayscale intensity functions of the reference and current images at location (x,y)
$(\widetilde{x}_{ref_i}, \widetilde{y}_{ref_i})$ and $(\widetilde{x}_{cur_i}, \widetilde{y}_{cur_i})$	the local coordinates at reference and current images
f_m and g_m	the mean grayscale values of reference and current images in the subset
S_s	the subset of DIC
λ_0	the wavelength of reflected signal (FBG)
n	the valid reflection coefficient of Bragg grating
Λ	the initial period of Bragg grating
ω	the strain transfer ratio

---

* Corresponding author.
E-mail addresses: zhang0@263.net, zhangguangqing@cup.edu.cn (G. Zhang).

https://doi.org/10.1016/j.enggeo.2018.09.016
Received 27 May 2018; Received in revised form 21 August 2018; Accepted 17 September 2018

λ	wavelength of reflected signal of deformed FBG sensor
ε_g	the strain of FBG sensor
ε_m	the strain of the specimen (FBG measured)
K_ε	the optical sensitive coefficient of strain
K_T	the optical sensitive coefficient of temperature
ΔT	the variation of temperature
r_m	the distance between the axis of fiber grating and the specimen surface
r_g	the fiber grating radius
E_g, E_c	the elastic modulus of fiber grating and coated layer
υ	the Poisson's ratio of the coated layer
H, S, B and a	height, span,thickness and notch length of the specimen
l_p and l_f	the lengths of fracture process zone and real fracture
σ	cohesive stress of the cohesive crack
δ	the crack opening displacement
δ_c	the critical crack opening displacement
σ_t	the cohesive tensile stress
b_1	slope of the soften curve of the cohesive crack model (material constant)
G_f	the dissipated energy in a unit zone
E_{ae}	AE energy
β	the proportionality between fracture energy and AE energy
δ_{ct}	crack tip opening displacement
l, L	developing and fully developed fracture process zone
G_D	the accumulated dissipated energy of FPZ
E_{Gae}	the accumulated AE energy in FPZ

1. Introduction

With the rapid development of civil infrastructures in urban areas and energy extraction from underground, the quality and safety of rock-like materials become a major concern. To facilitate mitigation of potential geological and anthropogenic hazards, advances in geophysical monitoring are desirable. Rock-like materials may exhibit a distinct non-linear zone surrounding the crack tip prior to failure (Zhang and Fan, 2016). This non-linear zone has been demonstrated to be the microcracks, i.e. the fracture process zone (Hoagland et al., 1973; Labuz et al., 1987), which disobeys the basic assumptions of linear elastic fracture mechanics (LEFM). Generally, the fracture of rock-like materials can be characterized by the cohesive crack model (Barenblatt, 1959; Dugdale, 1960; Hillerborg et al., 1976), including a real crack (traction-free zone) and a FPZ. The FPZ can be regarded as a cohesive crack, over which a distributed cohesive stress is acted and tends to close the FPZ. The fracture characteristics depicted by the cohesive crack model involves the interrelations of COD, FPZ length and cohesive fracture energy (maximum dissipated energy). However, no measurement technique can provide full information on rock fracturing characteristics in field applications.

The measurements of rock fracturing can be divided into indirect and direct approaches. For indirect approaches, most measurements are based on global responses of specimens, for instance the load-deflection or load-crack mouth opening displacement (Shah, 1990; Bažant and Xu, 1991). These indirect approaches cannot characterize any local responses around the crack tip, because they supply insufficient information of the predominant characteristics of rock fracturing. And direct approaches mainly include: optical (laser holography (Cai and Liu, 2009), speckle interferometry (Lin et al., 2009), visualization of microcracking (Backers et al. 2003), DIC (Chu et al., 1985; Roux et al., 2009), FBG (Zhu et al., 2015; Sun et al., 2016; Cao et al., 2018), etc.) and acoustical approaches (Kao et al., 2011; Ishida et al., 2017; Xing et al., 2017). Among them, AE and DIC seem more suitable for identifying rock fracturing. For AE, the sources and energy of AE events inside the specimen are used to determine FPZ dimensions, but the COD of cohesive crack in FPZ is not available. For DIC, the DIC-based surface displacement field is accessible for identifying COD and FPZ length, however, stress and dissipated energy during fracturing process is unobtainable. Therefore, characterization of AE and DIC can not be realized by AE or DIC individually, however, integration of AE and DIC can do. Despite this, there are still some limitations for both AE and DIC: (1) dependence on rigorous measuring conditions, (2) complicated post-test data processing, and (3) under par real-time measurement of rock fracturing, which limit the real-time application of rock fracturing in field application. Therefore, a new approach is needed to remedy the limitations of AE and DIC.

A relatively new technique, fiber Bragg grating, can identify the action of external fields (strain field and temperature field), by the variation of light wavelength in a grating region. In view of the limitations of the integrated measurement of AE and DIC, FBG seems to provide just the necessary complements, such as (1) weak sensitivity to experimental noise, (2) simple post-test data processing of specimen deformation, (3) reliable real-time measurement, etc. Currently, FBG is widely used to monitor the deformation inside and outside structures of various rock-like materials in civil engineering (Ni et al., 2013; Emadi et al., 2014), geological engineering (Sun et al., 2014; Gu et al., 2018), and petroleum engineering (Yang et al., 2017), etc. For rock fracture characterization, FBG-based measurement can be considered equivalent to DIC-based measurement, provided sufficient FBG sensors were deployed in a limited volume of rock mass. Since the number of sensors needed was confined to the limited detecting zone, sufficient placement of sensors is not easily realized with fiber Bragg grating technique. Thus, rock fracturing with limited number of FBG sensors was worth investigating.

In this paper, FBG, DIC and AE were combined to characterize the mode I fracturing process of sandstone. Measurement results showed a limited number of FBG sensors gave reliable rock fracturing characterization. The integration of three methods show more stable and real-time measurement, full-field surface displacements, and localized dissipated energy, etc. If COD, FPZ length and cohesive fracture energy can be recorded and analyzed in real-time, then the use of the cohesive crack model can be justified for both field and laboratory measurement. Field application of these integrated measurements can include engineering infrastructure (e.g., tunnels, roads, embankments) and geological hazards (e.g. landslides, active faults, cavities) in urban areas, as well as unconventional method of energy extraction from underground (Zhou et al., 2017; Zhou et al., 2018).

2. Principles and setup of the measurement methods (AE, DIC and FBG)

In this paper, mode I fracturing tests were performed on sandstone using three-point bending (3 PB), on a closed-loop, servo-hydraulic load system, at room temperature (20°C) and humidity (50 % RH), in which axial displacement control was applied at a rate of 0.01 mm/min. The fracturing process was simultaneously characterized by FBG, image and AE acquisition systems (Fig. 1).

2.1. Acoustic emission (AE)

2.1.1. Principles of AE-based measurement

Acoustic emission (AE) is defined as high-frequency elastic waves emitted from microcrack (Ishida et al., 2017), which takes place when the stored strain energy released is over the critical threshold. AE method is widely used to characterize the fracturing process of rock-like materials (Labuz et al., 1987; Xing et al., 2017; Kao et al., 2011). AE location is one of the most elementary variables for identifying FPZ. The